Macedonian Journal of Chemistry and Chemical Engineering, Vol. **41**, No. 1, pp. xx–xx (2022)

MJCCA9 –

ISSN 1857-5552
e-ISSN 1857-5625

Received: February 9, 2021
Accepted: May 17, 2022

DOI: 10.20450/mjcce.2022.2491
Original scientific paper

ESTABLISHING MASS SPECTRAL FRAGMENTATION PATTERNS FOR THE CHARACTERIZATION OF 1,2 -UNSATURATED PYRROLIZIDINE ALKALOIDS AND *N*-OXIDES IN *BORAGINACEAE* SPECIES FROM MACEDONIA USING LC-ESI-MS/MS

Jasmina Petreska Stanoeva*, Elena Stefova, Marinela Cvetanoska, Jane Bogdanov

Institute of Chemistry, Faculty of Natural Sciences and Mathematics,
Ss. Cyril and Methodius University in Skopje, Macedonia
jasmina.petreska@pmf.ukim.mk

Pyrrolizidine alkaloids (PAs) are secondary plant metabolites, and their 1,2-unsaturated derivatives, which contain the retronecine, heliotridine, or otonecine type of the necine base, have raised concern due to their ability to form hepatotoxic intermediates and exhibit serious toxic effects. Several hundred individual pyrrolizidine alkaloids and their *N*-oxides have been identified mostly using liquid chromatography coupled with mass spectrometry, although the number of available reference standards is limited.

In this work, characteristic fragment ions and their abundance in the mass spectra of different PAs were used to reveal typical fragmentation patterns for various classes of PAs that can be further employed to distinguish monoesters (retronecine, heliotridine type), open chain diesters and macrocyclic diesters, and corresponding *N*-oxides.

Fragment ions at *m/z* 120 and 138 were found in all types of PAs with a different relative abundance. Additional observation of fragment ions at *m/z* 94 and 156 was found to be typical for monoester PAs esterified at position C9 of the necin base, whereas fragment ions at *m/z* 111 and 172 were characteristic for monoester *N*-oxides. Fragment ions at *m/z* 180 and 220 were found to be typical for open chain diesters with esterification at C7 with acetic and angelic acid, respectively, whereas fragment ions at *m/z* 214 and 254 were characteristic for the respective *N*-oxides. For the 3′-acetyl PA monoester or open chain diester derivatives, characteristic fragment ions were observed after loss of the acetyl moiety ($[M+H]^+$–60), whereas for macrocyclic diesters and their *N*-oxides, fragment ions due to the neutral loss of CO were found ($[M+H]^+$–28).

Keywords: pyrrolizidine alkaloids and *N*-oxides; tandem mass spectrometry; *Boraginaceae*

ВОСПОСТАВУВАЊЕ НА МАСЕНОСПЕКТРОМЕТРИСКИ ФРАГМЕНТАЦИОНИ ПРОФИЛИ ЗА КАРАКТЕРИЗАЦИЈА НА 1,2-НЕЗАСИТЕНИ ПИРОЛИЗИДИНСКИ АЛКАЛОИДИ И *N*-ОКСИДИ ВО ВИДОВИ НА *BORAGINACEAE* ОД МАКЕДОНИЈА СО ПРИМЕНА НА LC-ESI-MS/MS

Пиролизидинските алкалоиди (ПА) се секундарни метаболити на растенијата, а нивните 1,2-незаситени дервати, кои содржат нецин-бази од типот на ретронецин, хелиотридин или отонецин, предизвикуваат загриженост поради способноста да формираат хепатотоксични интермедијари и да предизвикаат сериозни токсични ефекти. Досега, иако бројот на достапни референтни стандарди е ограничен, се идентификувани неколку стотици поединечни пиролизидински алкалоиди и нивни *N*-оксиди, главно со употреба на течна хроматографија спрегната со масена спектрометрија.

Во овој труд се користени карактеристичните фрагментни јони и нивната релативна застапеност во масените спектри на различни ПА, за да се откријат типични модели на фрагментацијата за различни класи на ПА кои можат понатаму да се користат за да се разликуваат моноестери (од типот на ретронецин, хелиотридин тип), диестери со отворена низа, макроциклични диестери, како и соодветните *N*-оксиди.

Фрагментните јони при *m/z* 120 и 138 се присутни кај сите типови на ПА со различна релативна застапеност. Дополнително е забележано дека присуството на фрагментни јони при *m/z* 94 и 156 е типично за моноестерските ПА, естерифицирани во позиција C9 на нецин-базата, додека фрагментните јони при *m/z* 111 и 172 се карактеристични за моноестерските *N*-оксиди. Утврдено е дека фрагментните јони при *m/z* 180 и 220 се типични за диестерите со отворена низа, кои во позиција C7 се естерифицирани со оцетна или ангелична киселина, соодветно, додека фрагментните јони при *m/z* 214 и 254 се карактеристични за соодветните *N*-оксиди. За 3′-ацетилните деривати на моноестерите или диестерите со отворена низа, карактеристични фрагментни јони се забележуваат по загуба на ацетилна група ($[M+H]^+$–60), додека за моноцикличните диестери и нивните *N*-оксиди е карактеристичен фрагментен јон кој се должи на неутрална загуба на CO ($[M+H]^+$–28).

Клучни зборови: пиролизидински алкалоиди и *N*-оксиди; тандемска масена спектрометрија; *Boraginaceae*

1. INTRODUCTION

In the last decade, there has been a growing interest in studying pyrrolizidine alkaloids (PAs) in the flowering plants of several plant families, especially ones from *Boraginaceae*, *Asteraceae*, and *Fabaceae*,[1] due to their demonstrated toxicity and their potential to enter the food chain.

PAs are a group of secondary metabolites produced by plants as their defense mechanism against herbivores. They are considered natural toxins that present a possible risk to humans because these toxic plant species are used in herbal teas or traditional medicines[2,3] or PAs can contaminate foods such as grain or grain products, honey, milk, tea, and beverages.[4,5]

The PAs and their *N*-oxides are esters of the necine base and necic acids. The necine base can either be saturated or contain a double bond in the 1,2-position, i.e., 1,2-unsaturated (Fig. 1). In general, saturated PAs are considered to be non-toxic,[6] whereas studies have demonstrated that 1,2-unsaturated PAs have hepatotoxic, genotoxic, cytotoxic, tumorigenic, and neurotoxic activities.[7,8]

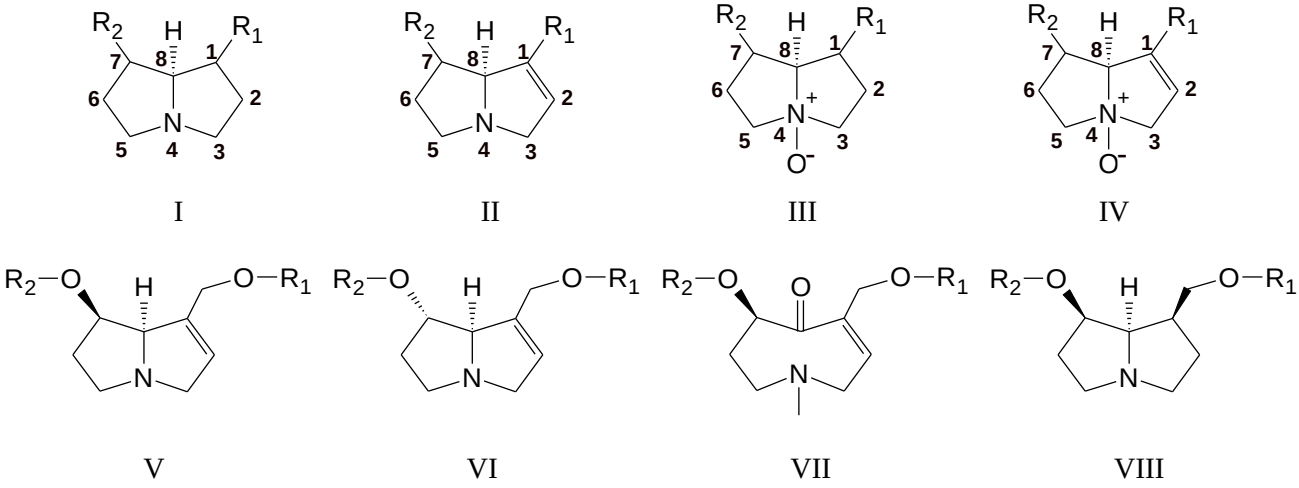

Fig. 1. General structure of heterocyclic tertiary amine-pyrrolizidine (I), 1,2-unsaturated pyrrolizidine (II) and the corresponding *N*-oxides (III and IV), and the four types of necine bases: retronecine (V), heliotridine (VI), otonecine (VII), and platynecine (VIII).

Depending on the chemical structure of the necine base, the unsaturated PAs can be further classified into retronecine, heliotridine, and otonecine type alkaloids (Fig. 1). Except for the otonecine type (that cannot form *N*-oxides), *N*-oxides of the other two types of PAs also naturally occur and often coexist with PAs in plants.

The necine base comprises two five-membered rings that share a nitrogen atom at position 4. In many cases, the necine base has a hydroxymethyl group at Cl and a hydroxyl group at C7. These hydroxyl groups can be esterified with necic acid(s), giving monoester (I), open-chain diester (II), or macrocyclic diester alkaloids (III) (Fig. 2).

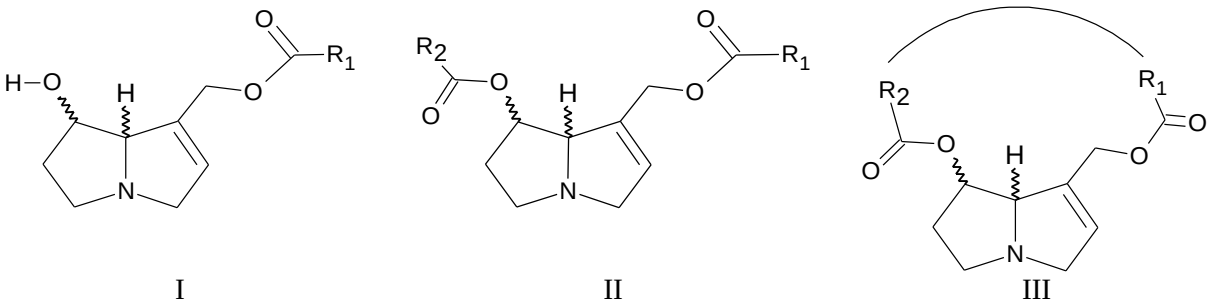

Fig. 2. Monoester (I), open-chain diester (II), and macrocyclic diester pyrrolizidine alkaloids

The necic acids found in PAs, excluding acetic acid, possess 5 to 10 carbon atoms. They can be mono- or dicarboxylic acids with branched carbon chains with hydroxy, epoxy, carboxy, acetoxy, methoxy, or other alkoxy groups as substituents.[9–11]

The exact number of naturally occurring PAs can only be estimated, but up to now, more than six hundred have been reported in the literature. The analytical standards of these natural products are not readily available, and their number is limited to less than thirty.[12] As a result of this discrepancy between the number of PAs described in the literature and the number of available standards, it is very difficult to identify and quantify different PAs in plant material and food products in order to perform a proper risk assessment. This kind of through assessment is becoming an important issue in food safety regulations. For that reason, it is necessary to find adequate tools by detecting characteristic markers that can be correlated to their structure and then used for structural characterization.

In the literature, several methodologies for the characterization of PAs can be found, including chromatographic separation techniques such as thin-layer chromatography (TLC), liquid chromatography (LC), and gas chromatography (GC) coupled with different detectors.[13] Capillary electrophoresis (CE) and miscellaneous electrokinetic chromatography (MEKC) techniques, which are based on a combination of electrophoretic and chromatographic principles,[14] have also been used. Additionally, specific techniques without prior separation or purification such as ^{1}H-NMR or ^{13}C-NMR were also used.[15]

In the last few years, chromatography coupled with mass spectrometry has become a methodology of choice for performing qualitative and quantitative analysis of PAs and their *N*-oxides (PANOs) as contaminants in plants and foods. However, in GC-MS analysis, the thermal decomposition of labile *N*-oxides or the deesterification of PAs was frequently observed.[16] Also, the analysis is time consuming due to the sample preparation with derivatization, and for these reasons, LC-MS methods are preferred and recommended.[17]

According to the National Report titled "Country Study for Biodiversity of the Republic of Macedonia",[18] the species *Echium italicum* L., *Echium vulgare* L., *Onosma* L. *heterophylla* Griseb., and *Symphytum officinale* L. from *Boraginaceae* are widespread in the country and could be a potential source of PAs that may present a risk factor in the food chain.

The aim of this work was to carry out a systematic investigation of the tandem mass spectral fragmentation patterns of PAs and PANOs on seventeen available reference compounds and to develop and implement an efficient strategy for the characterization of PAs and PANOs present in the above-mentioned *Boraginacea species* from Macedonia employing liquid chromatography coupled with an ion trap mass spectrometer as the detector and electrospray ionization (ESI).

2. EXPERIMENTAL

2.1. *Reagents and standards*

Methanol and ammonium formate (all LC-MS grade) were obtained from Sigma-Aldrich (St. Louis, MO, USA).

Seventeen available standards were used for the the analytical method development: europine-hydrochloride (Eu), europine-*N*-oxide (EuN), heliotrine (Hn), heliotrine-*N*-oxide (HnN), lycopsamine (La), lycopsamine-*N*-oxide (LaN), lasiocarpine (Lc), echimidine (Em), retrorsine (Re), retrorsine-*N*-oxide (ReN), senecionine (Sc), senecionine-*N*-oxide (ScN), seneciphylline (Sp), senecivernine (Sv), monocrotaline (Mc), monocrotaline-*N*-oxide (McN), and jacobine (Jb). All standards were purchased from Phytolab (Vestenbergsgreuth, Germany) and were used without further treatment/purification.

2.2. *Plant material*

Fourteen plant samples were collected in June 2021 in N. Macedonia. Seven samples were from the species *Echium vulgare* L (Katlanovska Brezica, Kozjak, Moroišta, Mavrovo (two locations), Volino (two locations), Kučkovo, Mešeišta), two samples from the species *Onosma heterophylla* Griseb. (Nova Breznica, Kozjak, Katlanovska Brezica), and one sample from each of the species *Echium italicum* L. (Galičica, s. Trpejca), *Cynoglossum creticum* Mill. (Katlanovska Brezica), and *Symphytum officinale* L. (Kumanovo, cultivated). Plant identity was verified by Academician Vlado Matevski.

Samples were collected in the period of full flowering without traces of soil, dust, or parts of other plants. Samples were air-dried in a place with good ventilation away from direct sunlight. Dry plant material was packed in paper bags and closed. The bags were stored at room temperature in a dry and dark place.

2.3. *LC-ESI-MS/MS analysis*

An Agilent 1100 HPLC system equipped with an ESI interface and an ion-trap mass analyzer (G2445A Spectrometer) controlled by LCMSD software (Agilent, v.4.1) was used to carry out the MS and MS^2 analysis. The samples were separated on a 150 mm × 2.1 mm, 2.7 μm Poroshell column (Agilent, USA). The mobile phase consisted of 5 mmol/l ammonium formate and 1 % formic acid in water (pH = 3.15) as a solvent A and 5 mmol/l ammonium formate and 1 % formic acid in methanol (pH = 4.88) as a solvent B. The gradient program started at 5 % B for 1 min, linearly increased to 35 % B to 10 min and then up to 80 % B from 10 to 20 min, isocratic 100 % B from 21 to 25 min, and finally decreased to 5 % B to 30 min and equilibrated for 10 min. The flow rate was 0.3 ml/min, and the injection volume was 5 μl.

The mass detector was equipped with an ESI system. The operation parameters in the positive ion mode were as follows: nebulizing gas (nitrogen) at a pressure of 50 psi and flow adjusted to 12 l/min, ion spray voltage of 3.5 kV, and capillary temperature of 325 °C. The full scan covered the mass range at *m/z* 15–600.

2.4. *Extraction procedure*

Approximately 100 g of plant material was homogenized, and precisely 2 g of powdered material was extracted with methanol (2 × 10 ml), ultrasonicated for 30 min (Branson model 3510, USA), and centrifuged for 15 min at 3500 RCF (Hettich EBA 200, USA). The supernatant was applied to the preconditioned C18 Sep-Pack cartridge with a 500 mg stationary phase (Waters, USA) with 5 ml of methanol and 5 ml of water and dried with 5 ml of air. 20 ml of the extract was loaded, and the sample cleanup was performed with 5 ml of water, followed by drying with 5 ml of air (two times). Elution was performed with 5 ml of methanol. Finally, the extract was filtered through a 0.45 μm filter (UPTIDISC RC 13 mm) before the analysis.

3. RESULTS AND DISCUSSION

Fragmentation patterns were studied by recording the MS and MS^2 spectra of the seventeen commercially available standards and twenty-four compounds extracted from the plants species of *Echium vulgare* L., *Echium italicum* L., *Onosma heterophylla* Griseb., *Cynoglossum creticum* Mill., and *Symphytum officinale* L., which are the more prevalent *Boraginaceae* species in Macedonia[18] and, therefore, present potential risk for food contamination.

Based on the observed MS fragmentation patterns of the available standards and literature data[19–22], it was deduced that alkaloids detected in the analyzed species can be characterized as monoesters (six of the retronecine type and five of the heliotridine type), open-chain diesters (nine of the retronecine type and one of the heliotridine type), and one macrocyclic diester (retronecine type) (Table 1).

PAs of a retronecine and heliotridine type are diastereoisomers at position C7 (Fig. 1), and their characterization in the MS spectra is based on the detection of fragment ions at *m/z* 120 and 138. Additional observation of fragment ions at *m/z* 94 and 156 provided the monoester PA, esterified at position C9 of the niacin base (Fig. 3). Due to the same fragmentation pattern exhibited by both these types (retronecine and heliotridine), they cannot be distinguished using only these fragments, but some differences in the relative abundance of fragments may be used to further distinguish them.

The fragment ion at *m/z* 138 is found in monoesters of both types of alkaloids with an abundance of up to 60 % or even as a base peak (100 %). The fragment ions at *m/z* 120 and 94 have a relative abundance mostly below 5 % in the heliotridine type, whereas their abundance is higher at up to 30 % and 50 % in the retronecine type of alkaloids, respectively (Table 2).

T a b l e 1

LC/ESI/MS-MS data for pyrrolizidine alkaloids from Boraginacae species and standards

No.	Compounds	Type	t_R/min	$[M+H]^+$	MS^2 (%, relative abundance)
Monoesters					
1	Rinderine[a]	H	16.7	300	282 (2), 156(5), **138** (100), 120 (5), 96(7), 94 (1)
2	3'-*O*-Acetyllycopsamine[a]	R	29.2	342	324 (50), **284** (100), 189 (15), 172 (5), 138 (30), 120 (20)
3	Lycopsamine[a,b]	R	17.0	300	256 (2), 210 (2), 156 (50), **138** (100), 120 (29), 94 (43)
4	Lycopsamine-*N*-oxide[a,b]	R	17.7	316	298 (4), 272 (11) 226 (25), **172** (100), 156 (5), 138 (56), 120 (2), 94 (8)
5	Echinatine[a]	H	21.1	300	282 (5), 256 (3), 156 (10), **138** (100), 120 (35), 110 (2), 94 (1)
6	Echinatine-*N*-oxide[a]	H	28.6	316	298 (11), 272 (4), 256 (46),**172** (100), 160 (4), 138 (3), 120 (1), 106 (50)
7	Heliotrine[a,b]	H	19.3	314	296 (1), 156 (4), **138** (100), 96 (7), 94 (2)
8	Heliotrine-*N*-oxide[a,b]	H	19.5	330	298 (2), **172** (100), 154 (1), 138 (3), 111 (2), 94 (2)
9	Europine[b]	H	12.4	330	312 (20), **254** (100), 156 (6), 138 (65), 120 (2), 96(5), 94 (3)
10	Europine-*N*-oxide[b]	H	17.4	346	**328** (100), 288 (6), 270 (41), 256 (20), 172 (42)
11	Lepthantine-*N*-oxide[a]	R	3.7	332	**314** (100), 276 (10), 270 (54), 256 (18), 228 (9), 172 (83), 138 (5), 120 (1), 111 (1)
12	7-Angeloylretronecine-*N*-oxide[a]	R	17.8	254	220 (3), 192 (10), 176 (8), 172 (1), 154 (31), 136 (60), **106** (100), 94 (1)
13	9-*O*-Angeloylretronecine-*N*-oxide[a]	R	20.5	254	238 (5), 192 (4), 154 (33), **138** (100), 120 (7), 111 (1), 94 (1)
Open-chain diester					
14	7-*O*-Acetyllycopsamine[a]	R	18.9	342	181 (2), **180** (100), 121 (3), 120 (4), 117 (5), 94 (2)
15	7-*O*-Acetyllycopsamine-*N*-oxide[a]	R	19.1	358	314 (5), 266 (10), **254** (100), 220 (5), 214 (50), 180 (10), 120 (2)
16	7-*O*-Acetylintermedine-*N*-oxide[a]	R	20.0	358	340 (7), 314 (12), 298 (20), 268 (15), **214** (100), 180 (8), 172 (6), 138 (5), 120 (6), 106 (3)
17	Uplandicine[a]	R	15.8	358	340 (20), 316(15), **298** (100), 220 (5),180 (15), 172 (45), 156 (5), 138 (3)
18	Uplandicine-*N*-oxide[a]	R	16.1	374	**356** (100), 312 (49), 298(7), 270(4), 254 (5), 220 (2), 214 (80), 180 (2), 172 (5)
19	3′-*O*-Acetylechiumine-*N*-oxide[a]	R	21.7	440	380 (10), 292 (5), 254 (2), **220** (100), 214 (10), 176 (3), 172 (10), 155 (5), 120 (1)
20	7-Angeloylechinatine[a]	H	21.5	382	372 (5), 238 (10), 220 (70), 136 (5), **120** (100), 119 (1)
21	Echiumine[a]	R	2.3	382	238 (15), **220** (100), 138 (10), 120 (35)
22	Echiumine-*N*-oxide[a]	R	23.5	398	354 (6), 308 (19), 298 (3), **254** (100), 237 (3), 220 (5), 214 (5), 190 (3), 120 (6)
23	Echimidine[a,b]	R	21.0	398	380 (8), **336** (100), 296 (4), 254 (5), 220 (10), 190 (3), 120 (2)
24	Lasiocarpine[b]	H	23.1	412	394 (20), 336 (60), 238 (4), 220 (100), 120 (21)
Macrocyclic diester					
25	Monocrotaline[a,b]	R	9.8	326	298 (9), **280** (100), 238 (23), 237 (27), 210 (9), 138 (2), 120 (25)
26	Monocrotaline-*N*-oxide[b]	R	12.0	342	314 (10), **296** (100), 253 (7), 236 (26), 209 (4), 138 (34), 120 (26)
27	Jacobine[b]	H	12.2	352	324 (4), **308** (100), 280 (58), 262 (32), 234 (8), 216 (4), 200 (8), 155 (23), 138 (5), 120 (16)
28	Retrorsine[b]	H	18.0	352	**324** (100), 306 (4), 280 (10), 276 (23), 151 (3) 138 (18), 120 (35)
29	Retrorsine-*N*-oxide[b]	H	18.4	368	**340** (100), 245 (6), 220 (10), 138 (50), 136 (20), 120 (20), 94 (30)
30	Seneciphylline[b]	H	19.5	334	**306** (100), 288 (18), 172, 151 (3), 138 (15), 120 (38), 94 (4)
31	Senecivernine[b]	H	19.8	336	**308** (100), 306 (10), 280 (5), 138 (22), 120 (35)
32	Senecionine[b]	H	19.7	336	**308** (100), 290 (11), 153 (3), 138 (19), 120 (41)
33	Senecionine-*N*-oxide[b]	H	19.9	352	334 (6), **324** (100), 254 (23), 246 (47), 220 (70), 202 (12), 178 (4), 156 (7), 136 (29), 118 (74)

[a]identified in plant material, [b]available as standard, R – retronecine, H – heliotridine

(A) Monoesters

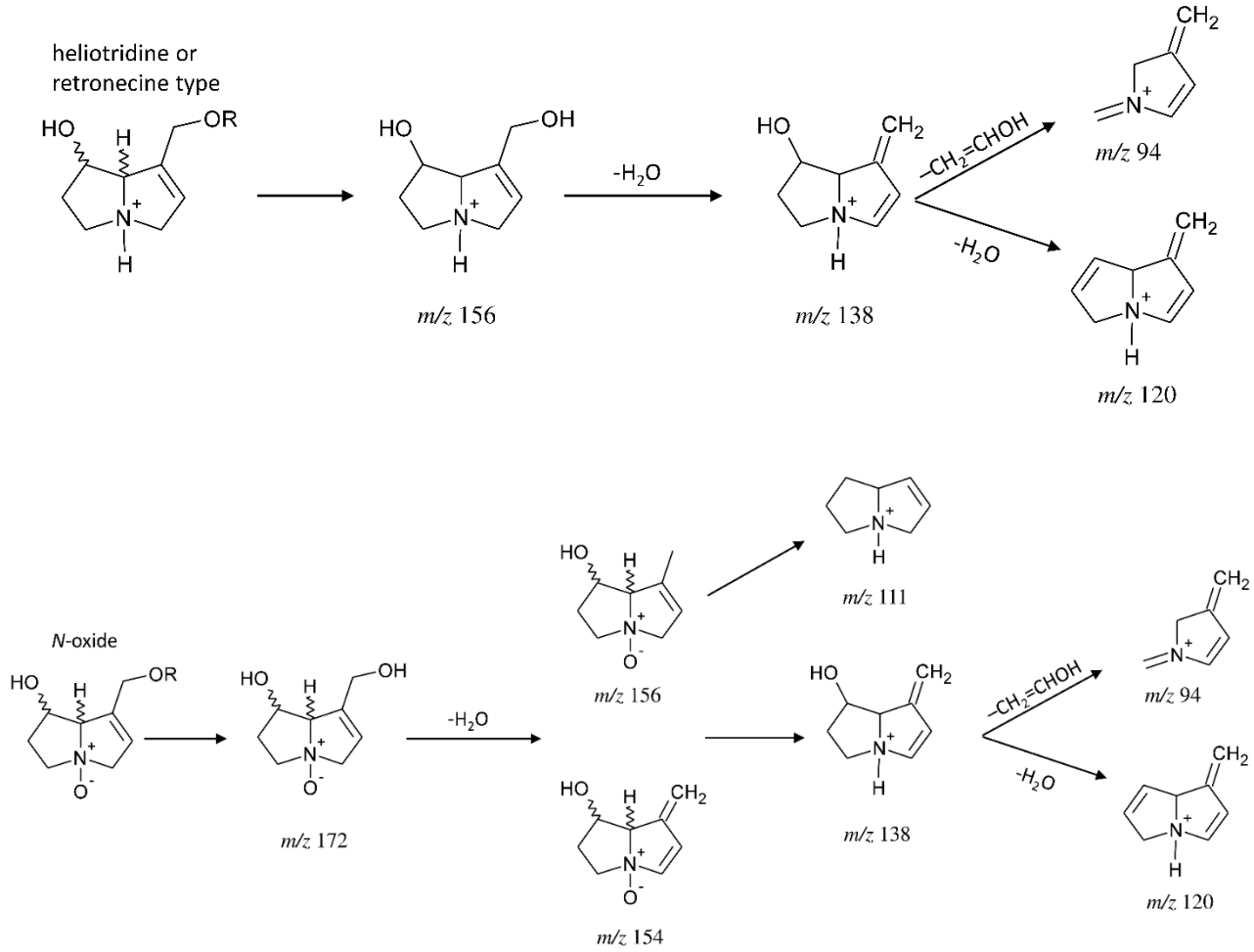

(B) Open chain diesters

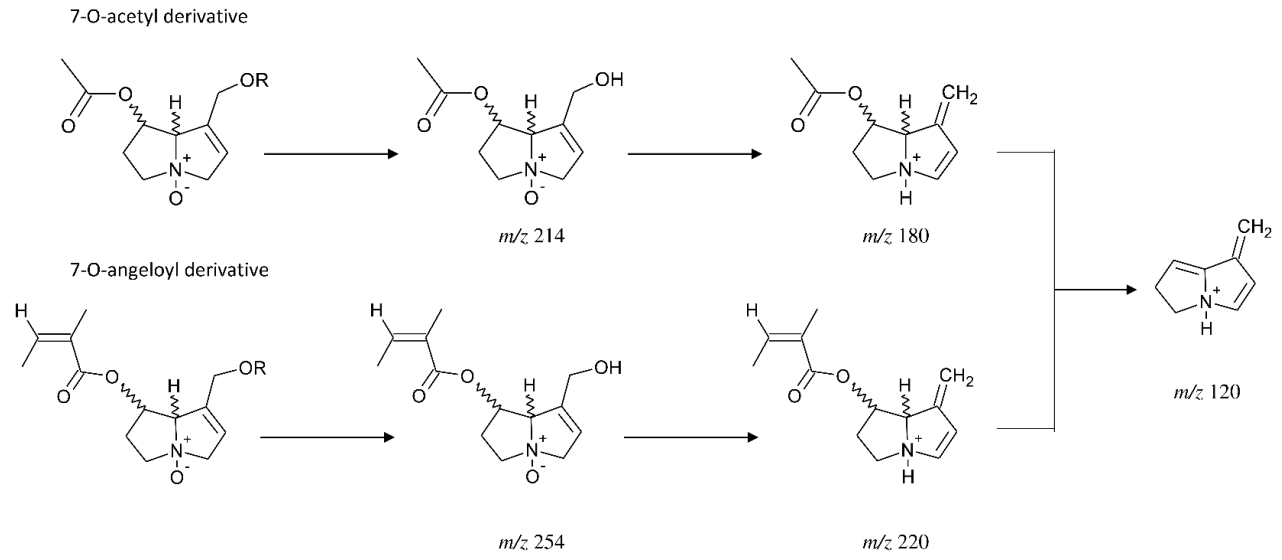

Fig. 3 (A, B)

(C) Macrocyclic diesters

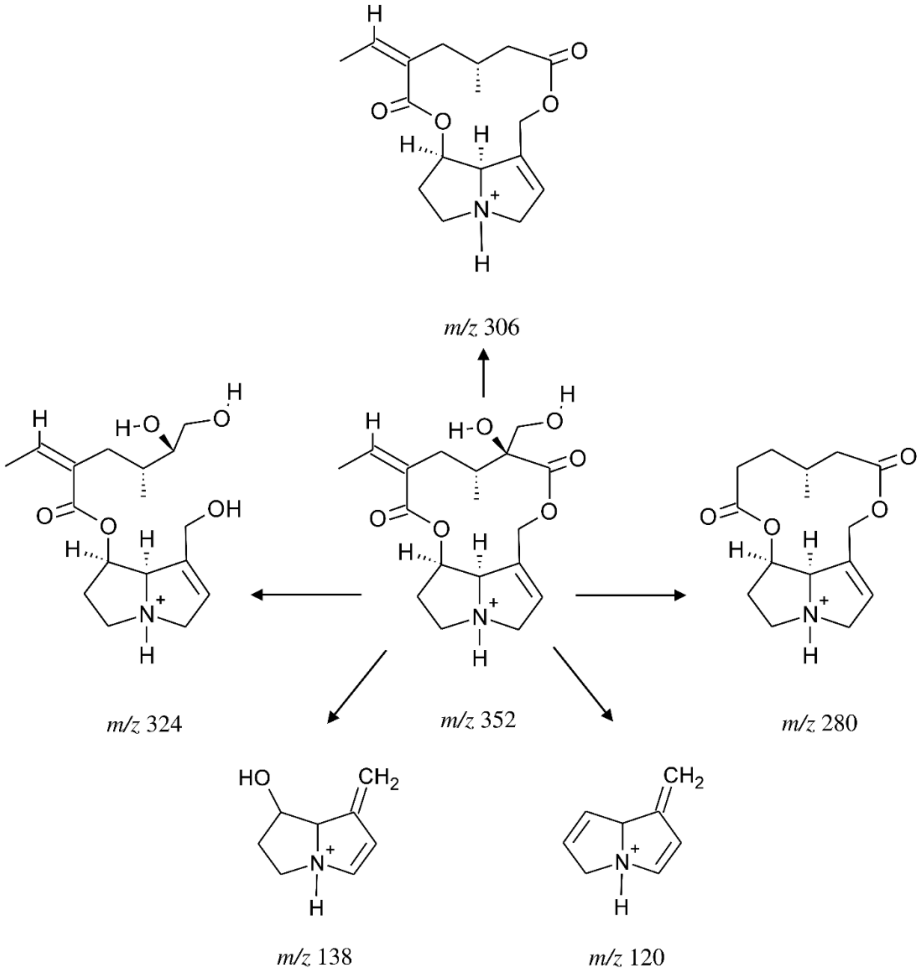

Fig. 3 (C)

Fig. 3. General fragmentation pathway of (A) monoesters, (B) open chain diesters, and (C) macrocyclic diesters

T a b l e 2

Characteristic mass spectrometric fragment ions and respective relative intensity ratio (%) used for screening and confirmation of PAs and PANOs of different base and ester types

	m/z $[M+H]^+$							
1,2 unsaturated necine base	94	111	120	136	138	156	172	256
O^9-monoester								
retronecine	5		5		100	50		
heliotridine	50		30		100	5		
O^9-monoester *N*-oxide								
retronecine		2			50		100	20
heliotridine		1			5		100	20
Open chain diester								
retronecine			5		5			
heliotridine			100		1			
Open chain diester *N*-oxide				5	5			
Macrocyclic diester			35		20			
Macrocyclic diester *N*-oxide				30	20			

According to the fragmentation pattern, one monoester of the retronecine type (lycopsamine (**3**)) and three monoesters of the heliotridine type (rinderine (**1**), echinatine (**5**), and heliotrine (**7**)) were identified in the analyzed samples (Fig. 3). The MS^2 spectra of all analyzed monoesters and their *N*-oxides are presented in Figure 4.

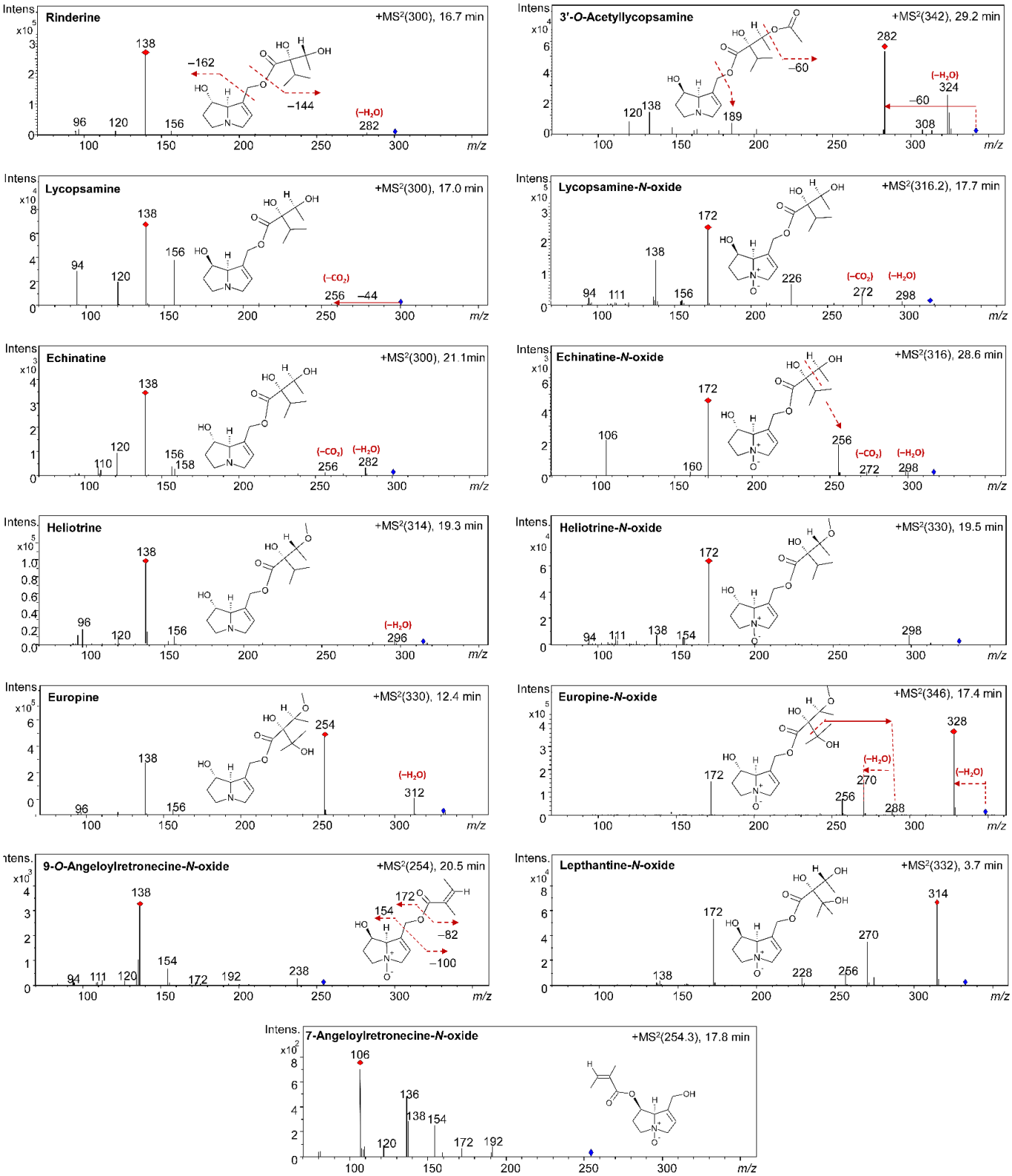

Fig. 4. MS^2 spectra of analyzed monoesters and their *N*-oxides

Lycospamine (**3**) was found in extracts of *E. vulgare* L. and *S. officinale* L., and rinderine (**1**) and echinatine (**5**) were found in extracts of *C. creticum* Mill., whereas heliotrine (**7**) was detected in *E. vulgare* L. In the literature, lycospamine (**3**) was also found in *E. vulgare* L., *E. hupertropicum* L., *E. plantagineum*, and *S. officinale* L.,[23–25] rinderine (**1**) was found in *C. officinale* L.,[25] and echinatine (**5**) was found in *C. officinale* L. and *S. officinale* L.,[25] whereas heliotrine (**7**) was not previously detected in the *Boraginacae* species.

The acetylated moiety of 3′-*O*-acetyllycopsamine (**2**) found in *E. italicum* was confirmed by the peak at *m/z* 282 as the most abundant fragment that is obtained after a loss of acetic acid ($[M+H]^+$–60), as shown in Figure 4. Previously, this compound was detected only in *E. hypertropicum* L.[24]

In the corresponding *N*-oxides (O^9-monoester *N*-oxide), additional fragment ions at *m/z* 111 and 172 were observed. The fragment ion at *m/z* 172 is abundant at up to 50 % or 100 % in both the retronecine and heliotridine type of *N*-oxides. Another characteristic fragment ion for PAs at *m/z* 138 was also found in the monoester *N*-oxides of the retronecine type with a relative abundance up to 50 %, whereas in the heliotridine type, it was below 5 % (Table 2).

The *N*-oxides of lycopsamine (**4**), echinatine (**6**), heliotrine (**8**), and lepthantine (**11**) were also detected in the analyzed samples, and their MS^2 spectra are given in Fig. 4. Lycopsamine *N*-oxide (**4**) was found in the extracts of all analyzed species except in the extract of *E. italicum*. Echinatine *N*-oxide (**6**) was found in the extract of *E. italicum*. Heliotrine *N*-oxide (**8**) was found in one sample of *E. vulgare* L., whereas lepthantine *N*-oxide (**11**) was detected in the extracts of *E. vulgare* L., *O. heterophylla* Griseb, and *C. creticum* Mill. Lycopsamine *N*-oxide (**4**) and lepthantine *N*-oxide (**11**) were previously described in *E. vulgare* L. and *E. plantagenium* L.,[19,25,26] and echinatine *N*-oxide (**6**) was found in *S. officinale* L.,[25] whereas heliotrine *N*-oxide (**8**) was not previously detected in the corresponding species.

In the samples of *E. vulgare* L., two additional peaks with *m/z* 254 were detected (Fig. 4). Based on the observed MS fragmentation, it was deduced that both alkaloids are of the retronecine type and are monoesters with angelic acid at either C9 or C7. Based on the presence of fragment ions at *m/z* 220 and 106, both typical for C7 monoesters of the angelic acid type,[27] it is proposed that the peak at 17.8 min is due to the presence of 7-angeloylretronecine-*N*-oxide (**12**). The presence of fragment ions at *m/z* 238 ($[M+H]^+$–16), 154 ($[M+H]^+$–100), and 138 ($[M+H]^+$–16–100) for the peak with the retention time of 20.5 min implies that it is probably due to the other isomer, i.e., 9-*O*-angeloylretronecine-*N*-oxide (**13**). These two compounds were previously described in *E. vulgare* L., *E. plantagenum* L., *E. setosium* L., and *C. officinale* L.[19,25,26,28]

The MS data obtained for the analyzed samples indicate the presence of six open chain diesters (**14**, **17**, **20**, **21**, **23**, **24**) and five corresponding *N*-oxides (**15**, **16**, **18**, **19**, **22**) (Table 1, Fig. 5). The differentiation between the retronecine and heliotridine base was deduced from the characteristic intensity ratios of certain fragment ions at *m/z* 120 and 138. In the heliotrine type open chain diesters, the fragment ion at *m/z* 120 is 100%, whereas in the retronecine type, it is below 5% (Table 2).

In the MS^2 spectra of open chain diesters with esterification at C7 with acetic acid, one additional fragment ion at *m/z* 180 was observed (**14–16**), and a fragment ion at *m/z* 214 was observed for the respective *N*-oxide (**15, 16**). The analogous fragment ion at *m/z* 220 was observed for open chain diesters esterified with angelic acid (**17–24**), and the fragment ion at *m/z* 254 was observed for the corresponding *N*-oxide (Fig. 3B).[19] For 3′-acetylechiumine *N*-oxide (**20**), one additional fragment ion at *m/z* 380 was observed due to the loss of the acetyl moiety ($[M+H]^+$–60).

In the extracts of the analyzed plant samples, 7-*O*-acetyllycopsamine (**14**) and 7-*O*-acetylintermedine-*N*-oxide (**16**) were detected in *S. officinale* L., 7-*O*-acetyllycopsamine-*N*-oxide (**15**) and 7-angeloylechinatine (**20**) were detected in *E. vulgare* L., uplandicine and its *N*-oxide (**17**, **18**) were detected in *E. vulgare* L., *O. heterophylla* Griseb, and *C. creticum* Mill., 3′-*O*-acetylechiumine-*N*-oxide (**19**) was detected in *E. italicum* L., echiumine (**21**) was detected in all analyzed samples (except *S. officinale* L.), and its *N*-oxide (**22**) was detected in *E. vulgare* L. and *E. italicum* L. In the literature, 7-*O*-acetyllycopsamine-*N*-oxide (**15**) and 3′-*O*-acetylechiumine-*N*-oxide (**19**) were previously detected only in *E. vulgare* L.,[25] 7-*O*-acetyllycopsamine (**14**), uplandicine and its *N*-oxide (**17**, **18**), and echiumine *N*-oxide were detected in *E. vulgare* L., *E. plantagenium* L., and *S. officinale* L.[19,25,26], and echiumine (**21**) was detected in *E. vulgare L.* and *S. officinale* L.,[25] whereas 7-*O*-acetylintermedine-*N*-oxide (**16**) and 7-angeloylechinatine (**20**) were detected in *S. officinale* L. and *C. officinale* L.,[25] respectively.

In the MS^2 spectra of macrocyclic diesters and their *N*-oxides, fragment ions due to the neutral loss of CO (–28 amu) were detected. This loss

was not observed in the MS^2 spectra of monoesters or open chain diesters (Fig. 3C and Fig. 6). It is only characteristic for macrocyclic diesters and often gives the peak with the highest intensity in MS^2 like in compounds **28**, **29**, **30**, **31**, **32**, **33**, but it is also detected in the MS^2 spectra of compounds **25**, **26**, **27**. Additionally, the fragment ions at *m/z* 120 and 138, due to the necine base, were also observed with a relative abundance of up to 20 % (Table 2).

In the extracts of the studied plant samples, only monocrotaline (**25**) was detected in *E. italicum* L. (Table 1). Macrocyclic PAs are not characteristic for the *Boraginaceae* species, and in the literature[1,29], there is no available data about their presence in the corresponding *Boraginacae* species.

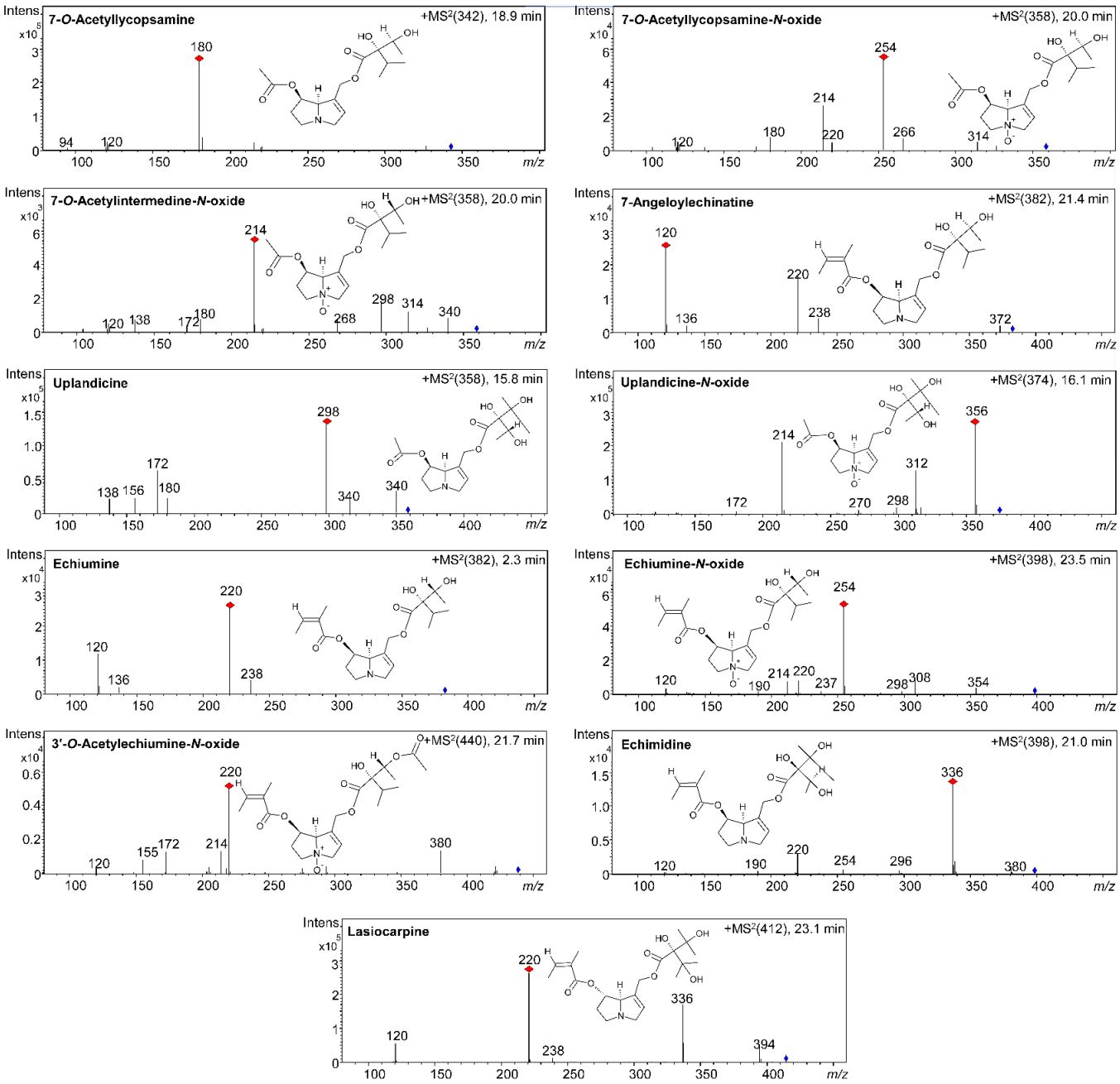

Fig. 5. MS^2 spectra of the analyzed open chain diesters and their *N*-oxides

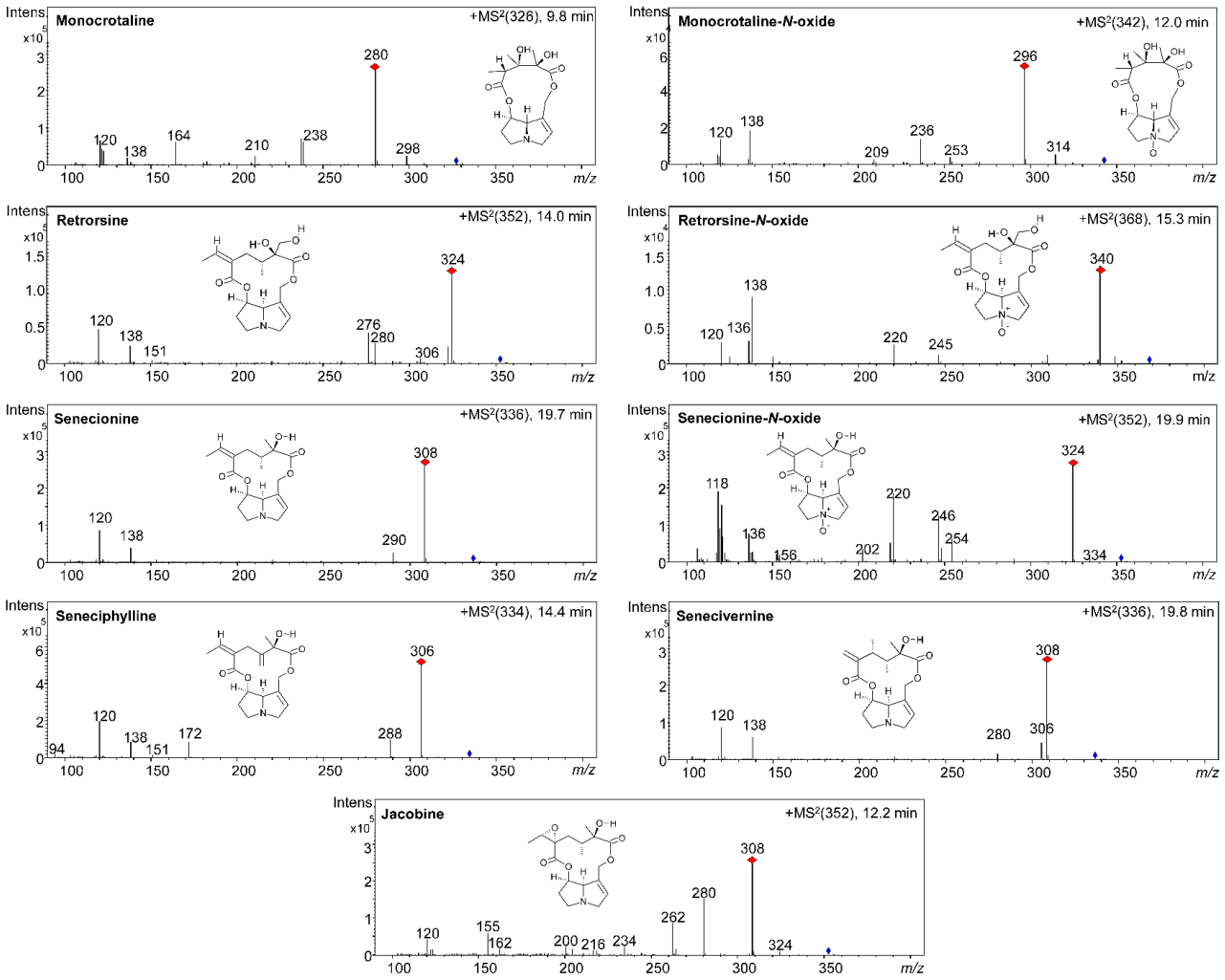

Fig. 6. MS^2 spectra of the analyzed macrocyclic diesters and their *N*-oxides

4. CONCLUSION

Pyrrolizidine alkaloids (PAs) and pyrrolizidine alkaloids *N*-oxides with 1,2-unsaturated derivatives that contain the retronecine, heliotridine, or otonecine type of the necine base can be conveniently characterized with electrospray ionization (ESI) using (tandem) mass spectral fragmentation patterns. In this systematic study that utilized LC-ESI-MS/MS, characteristic fragment ions and their abundance in the mass spectra of different standards of PAs and PANOs were used to reveal typical fragmentation patterns for various classes of PAs. The obtained results were further employed to distinguish monoesters (retronecine, heliotridine type), open chain diesters, and macrocyclic diesters and corresponding *N*-oxides. Utilizing this method, PAs and the corresponding PANOs can easily be differentiated, and moreover, characterization of these compounds in the abscence of analytical standards can be carried out. With the mass spectral fragmentation patterns, the PA profiles of several plants from the *Boraginaceae* species from N. Macedonia were obtained. The developed method (extraction, purification, separation, and characterization) can be conveniently used for the characterization of PAs and PANOs in various plants, and with a slight modification, it can be used to detected their presence in various food products.

Acknowledgements. The authors gratefully acknowledge the financial support provided by the OPCW for the project titled: "Risk Analysis of Natural Toxic Pyrrolizidine Alkaloids in the Food Chain: Development, Validation, and Application of HPLC/MS^n Methods", Grant L/ICA/ICB/222477/20.

REFERENCES

(1) El-Shazly, A.; Wink, M., Diversity of pyrrolizidine alkaloids in the Boraginaceae structures, distribution, and biological properties. *Diversity* **2014**, *6* (2), 188–282. https://doi.org/10.3390/d6020188.

(2) Chen, L.; Mulder, P. P. J.; Peijnenburg, A.; Rietjens, I. M. C. M., Risk assessment of intake of pyrrolizidine alkaloids from herbal teas and medicines following realistic exposure scenarios. *Food Chem. Toxicol.* **2019**, *130* (May), 142–153. https://doi.org/10.1016/j.fct.2019.05.024.

(3) Zuckerman, M.; Steenkamp, V.; Stewart, M. J., Hepatic veno-occlusive disease as a result of a traditional remedy: confirmation of toxic pyrrolizidine alkaloids as the cause, using an in vitro technique. *J. Clin. Pathol.* **2002**, *55* (9), 676–679. https://doi.org/10.1136/jcp.55.9.676.

(4) Reinhard, H.; Zoller, O., Pyrrolizidine alkaloids in tea, herbal tea and iced tea beverages – survey and transfer rates. *Food Addit. Contam.* Part A *Chem. Anal. Control Expo. Risk Assess.* **2021**, *38* (11), 1914–1933. https://doi.org/10.1080/19440049.2021.1941302.

(5) Casado, N.; Morante-Zarcero, S.; Sierra, I., The concerning food safety issue of pyrrolizidine alkaloids: an overview. *Trends Food Sci. Technol.* **2022**, *120*, 123–139. https://doi.org/10.1016/j.tifs.2022.01.007.

(6) Moreira, R.; Pereira, D. M.; Valentão, P.; Andrade, P. B., Pyrrolizidine alkaloids: chemistry, pharmacology, toxicology and food safety. *Int. J. Mol. Sci.* **2018**, *19* (6). https://doi.org/10.3390/ijms19061668.

(7) He, Y.; Zhu, L.; Ma, J.; Lin, G., Metabolism-mediated cytotoxicity and genotoxicity of pyrrolizidine alkaloids. *Arch. Toxicol.* **2021**, *95* (6), 1917–1942. https://doi.org/10.1007/s00204-021-03060-w.

(8) Teschke, R.; Vongdala, N.; Quan, N. Van; Quy, T. N.; Xuan, T. D., Metabolic toxification of 1,2-unsaturated pyrrolizidine alkaloids causes human hepatic sinusoidal obstruction syndrome: the update. *Int. J. Mol. Sci.* **2021**, *22* (19), 1–43. https://doi.org/10.3390/ijms221910419.

(9) El-Shazly, A.; Wink, M., Diversity of pyrrolizidine alkaloids in the Boraginaceae structures, distribution, and biological properties. *Divers.* **2014**, *6* (2), 188–282. https://doi.org/10.3390/d6020188.

(10) Prada, F.; Stashenko, E. E.; Martínez, J. R. LC/MS Study of the diversity and distribution of pyrrolizidine alkaloids in Crotalaria species growing in Colombia. *J. Sep. Sci.* **2020**, *43* (23), 4322–4337. https://doi.org/10.1002/jssc.202000776.

(11) Schramm, S.; Köhler, N.; Rozhon, W., Pyrrolizidine alkaloids: biosynthesis, biological activities and occurrence in crop plants. *Molecules* **2019**, *24* (3). https://doi.org/10.3390/molecules24030498.

(12) Wiedenfeld, H.; Pyrrolizidine alkaloids. In: *Encyclopedia of Toxicology* (Third edition), Academic Press: Oxford, 2014; pp 1170–1174. https://doi.org/10.1016/B978-0-12-386454-3.00054-3.

(13) Crews, C., Methods for analysis of pyrrolizidine alkaloids. In: Ramawat K., Mérillon JM. (Eds.) *Natural Products*.; Springer, Berlin, Heidelberg, 2013; pp 1050–1065. https://doi.org/10.1007/978-3-642-22144-6_186.

(14) Gotti, R., Analysis of alkaloids by capillary electrophoresis. In: Ramawat K., Mérillon JM. (Eds.) *Natural Products*.; Springer, Berlin, Heidelberg 2013; pp 1155–1992. https://doi.org/10.1007/978-3-642-22144-6_190.

(15) Kopp, T.; Abdel-Tawab, M.; Mizaikoff, B., Extracting and analyzing pyrrolizidine alkaloids in medicinal plants: A review. *Toxins (Basel).* **2020**, *12* (5), 7–10. https://doi.org/10.3390/toxins12050320.

(16) Mroczek, T.; Glowniak, K.; Wlaszczyk, A. Simultaneous determination of N-oxides and free bases of pyrrolizidine alkaloids by cation-exchange solid-phase extraction and ion-pair high-performance liquid chromatography. *J. Chromatogr. A* **2002**, *949* (1–2), 249–262. https://doi.org/10.1016/S0021-9673(01)01498-4.

(17) *Bestimmung von Pyrrolizidinalkaloiden (PA) in Pflanzenmaterial mittels SPE-LC-MS/MS. Methoden-beschreibung*. BfR – Bundesinstitut für Risikobewertung **2014**, 1–17.

(18) *Country Study for Biodiversity of the Republic of Macedonia* (First National Report). *Museum* **2003**.

(19) Colegate, S. M.; Edgar, J. A.; Knill, A. M.; Lee, S. T., Solid-phase extraction and HPLC-MS profiling of pyrrolizidine alkaloids and their *N*-oxides: A case study of *Echium* plantagineum. *Phytochem. Anal.* **2005**, *16* (2), 108–119. https://doi.org/10.1002/pca.828.

(20) Lu, A.-J.; Lu, Y.-L.; Tan, D.-P.; Qin, L.; Ling, H.; Wang, C.-H.; He, Y.-Q., Identification of pyrrolizidine alkaloids in *Senecio* plants by liquid chromatography – mass spectrometry. *J. Anal. Methods Chem.* **2021**, 1957863. https://doi.org/10.1155/2021/1957863.

(21) Ruan, J.; Li, N.; Xia, Q.; Fu, P. P.; Peng, S.; Ye, Y.; Lin, G., Characteristic ion clusters as determinants for the identification of pyrrolizidine alkaloid *n*-oxides in pyrrolizidine alkaloid-containing natural products using HPLC-MS analysis. *J. Mass Spectrom.* **2012**, *47* (3), 331–337. https://doi.org/10.1002/jms.2969.

(22) Qi, X.; Wu, B.; Cheng, Y.; Qu, H., Simultaneous characterization of pyrrolizidine alkaloids and *N*-oxides in Gynura Segetum by liquid chromatography/ion trap mass spectrometry. *Rapid Commun. Mass Spectrom.* **2009**, *23* (2), 291–302. https://doi.org/10.1002/rcm.3862.

(23) Sixto, A.; Pérez-Parada, A.; Niell, S.; Heinzen, H., GC–MS and LC–MS/MS workflows for the identification and quantitation of pyrrolizidine alkaloids in plant extracts, a case study: *Echium Plantagineum*. *Rev. Bras. Farmacogn.* **2019**, *29* (4), 500–503. https://doi.org/10.1016/j.bjp.2019.04.010.

(24) Carvalho, J. C. B.; Dos S. Almeida H.; Lobo, J. F. R.; Ferreira, J. L. P.; Oliveira, A. P.; Rocha, L., Pyrrolizidine alkaloids in two endemic capeverdian *Echium* species. *Biochem. Syst. Ecol.* **2013**, *50*, 1–6. https://doi.org/10.1016/j.bse.2013.03.026.

(25) Mädge, I.; Gehling, M.; Schöne, C.; Winterhalter, P.; These, A., Pyrrolizidine alkaloid profiling of four Boraginaceae species from Northern Germany and implications for the analytical scope proposed for monitoring of maximum levels. *Food Addit. Contam.* Part A: *Chem. Anal. Control. Expo. Risk Assess.* **2020**, *37* (8), 1339–1358. https://doi.org/10.1080/19440049.2020.1757166.

(26) Skoneczny, D.; Weston, P. A.; Zhu, X.; Gurr, G. M.; Callaway, R. M.; Weston, L. A., Metabolic profiling of pyrrolizidine alkaloids in foliage of two *Echium* spp. Invaders in Australia — A case of novel weapons? *Int. J. Mol. Sci.* **2015**, *16* (11), 26721–26737. https://doi.org/10.3390/ijms161125979.

(27) El-Shazly, A.; Sarg, T.; Witte, L.; Wink, M., Pyrrolizidine alkaloids from *Cynoglossum creticum*. *Phytochemistry* **1996**, *42* (4), 1217–1221. https://doi.org/10.1016/0031-9422(96)00112-4.

(28) El-Shazly, A.; Sarg, T.; Ateya, A.; Abdel Aziz, A.; El-Dahmy, S.; Witte, L.; Wink, M., Pyrrolizidine alkaloids from *Echium setosum* and *Echium vulgare*. *J. Nat. Prod.* **1996**, *59* (3), 310–313. https://doi.org/10.1021/np9600661.

(29) Schramm, S.; Köhler, N.; Rozhon, W., Pyrrolizidine alkaloids: biosynthesis, biological activities and occurrence in crop plants. *Molecules* **2019**, *24* (3), 1–44. https://doi.org/10.3390/molecules24030498